

Thermodynamic and Exergoeconomic Assessment of a Solar-Assisted Combined Cooling, Heating, and Power System in Antalya, Turkey

Abdulrazzak AKROOT^{1*} , and Mohammed REFAEI¹ 

¹Karabük University, Faculty of Engineering, Department of Mechanical Engineering, Karabük, Turkey

Article Info

Research article
Received: 26/11/2024
Revision: 08/01/2025
Accepted: 05/02/2025

Keywords

Solar-Assisted Energy Systems
Organic Rankine Cycle
Exergoeconomic analysis
Parabolic trough collectors

Makale Bilgisi

Araştırma makalesi
Başvuru: 26/11/2024
Düzeltilme: 08/01/2025
Kabul: 05/02/2025

Anahtar Kelimeler

Güneş Destekli Enerji Sistemleri
Organik Rankine Döngüsü
Eksergoekonomik analiz
Parabolik oluk kolektörleri

Graphical/Tabular Abstract (Grafik Özet)

This study evaluates a solar-assisted CCHP system, finding R245fa more efficient and butane more cost-effective, supporting its viability in solar-rich regions like Antalya, Turkey/Bu çalışma, güneş destekli bir CCHP sistemini değerlendirerek R245fa'nın daha verimli, bütanın ise daha maliyet etkin olduğunu belirlemiştir ve Antalya gibi güneş zengini bölgeler için uygunluğunu göstermektedir.

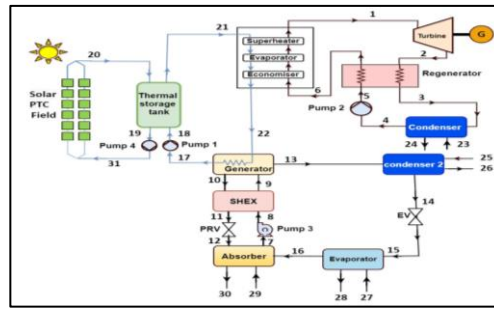


Figure A: The schematic diagram for the solar-assisted CCHP system (Güneş destekli CCHP sisteminin şematik diyagramı)

Highlights (Önemli noktalar)

- Thermodynamic and exergoeconomic analyses are conducted to evaluate the performance of a solar-assisted CCHP system in Antalya, Turkey/Antalya, Türkiye'deki güneş destekli CCHP sisteminin performansını değerlendirmek için termodinamik ve eksergoekonomik analizler gerçekleştirilmiştir.
- The impact of working fluids (R245fa and butane) on efficiency, cost, and environmental performance is assessed using steady-state simulations/Çalışma akışkanlarının (R245fa ve bütan) verimlilik, maliyet ve çevresel performans üzerindeki etkisi durağan hal simülasyonları kullanılarak değerlendirilmiştir.
- Exergoeconomic factors are analyzed to optimize system components, ensuring economic feasibility and sustainability/Sistem bileşenlerini optimize etmek, ekonomik fizibiliteyi ve sürdürülebilirliği sağlamak için eksergoekonomik faktörler analiz edilmiştir.

Aim (Amaç): This study aims to enhance the performance of solar-assisted CCHP systems by optimizing energy efficiency and reducing environmental impact through exergoeconomic analysis/Bu çalışma, eksergoekonomik analiz yoluyla enerji verimliliğini artırarak ve çevresel etkiyi azaltarak güneş destekli CCHP sistemlerinin performansını iyileştirmeyi amaçlamaktadır.

Originality (Özgünlük): This study assesses a solar-assisted CCHP system, comparing R245fa and butane for efficiency and cost-effectiveness to optimize sustainable energy solutions/Bu çalışma, güneş destekli CCHP sistemini değerlendirerek R245fa ve bütan verimlilik ve maliyet açısından karşılaştırmaktadır

Results (Bulgular): R245fa achieves higher efficiency (86.89%) and lower CO₂ emissions (0.195 kg/kWh), while butane reduces costs (63.06 \$/h). The 72.12% exergoeconomic factor supports R245fa's superior performance for sustainable solar-assisted CCHP systems/R245fa daha yüksek verimlilik (%86,89) ve düşük CO₂ emisyonu (0,195 kg/kWh) sağlarken, bütan maliyeti düşürmektedir (63,06 \$/saat). %72,12 eksergoekonomik faktör değeri, güneş destekli CCHP sistemlerinde R245fa'nın üstün performansını desteklemektedir.

Conclusion (Sonuç): This study confirms the efficiency of solar-assisted CCHP systems, showing R245fa as environmentally superior with higher efficiency, while butane is more cost-effective/Bu çalışma, güneş destekli CCHP sistemlerinin verimliliğini doğruluyor; R245fa çevresel açıdan üstünken, bütan daha maliyet etkindir.



Thermodynamic and Exergoeconomic Assessment of a Solar-Assisted Combined Cooling, Heating, and Power System in Antalya, Turkey

Abdulrazzak AKROOT^{1*} and Mohammed REFAEI¹

¹Karabük University, Faculty of Engineering, Department of Mechanical Engineering, Karabük, Turkey

Article Info

Research article
Received: 26/11/2024
Revision: 08/01/2025
Accepted: 05/02/2025

Keywords

Solar-Assisted Energy Systems
Organic Rankine Cycle
Exergoeconomic analysis
Parabolic trough collectors

Abstract

This study investigates the potential of solar-assisted combined cooling, heating, and power (CCHP) systems to address energy efficiency and sustainability challenges, particularly in regions with abundant solar resources, such as Antalya, Turkey. The thermodynamic design and exergoeconomic analysis were conducted on a tri-generation system that integrates parabolic trough collectors, an organic Rankine cycle engine, and an absorption refrigeration unit. Using steady-state simulations in the Engineering Equation Solver (EES), the analysis evaluated key performance metrics such as thermal and exergy efficiencies, power outputs, and cost rates for two working fluids: R245fa and butane. Results showed that the R245fa-based system achieved an electrical output of 232.5 kW, a cooling capacity of 716.7 kW, a heating capacity of 2225 kW, a thermal efficiency of 86.89%, an exergy efficiency of 16.26%, a total cost rate of 66.12 \$/h, and a carbon footprint of 0.195 kg CO₂/kWh. Additionally, the exergoeconomic factor for this system was 72.12%. On the other hand, the butane-based system produced 221.8 kW of electricity, 745.4 kW of cooling, and 2197 kW of heating, with a thermal efficiency of 86.44%, an exergy efficiency of 15.73%, a total cost rate of 63.06 \$/h, and a carbon footprint of 0.223 kg CO₂/kWh. The exergoeconomic factor for the butane-powered system was calculated at 70.86%. The Mean Absolute Percentage Error (MAPE) for the model validation was less than 5%, confirming the reliability of the results. The findings emphasize the superior performance of R245fa in terms of thermodynamic and environmental metrics, while butane offers cost advantages.

Antalya'da Güneş Enerjisiyle Çalışan Kombine Soğutma, Isıtma ve Güç Sisteminin Termodinamik ve Eksergoekonomik Değerlendirmesi

Makale Bilgisi

Araştırma makalesi
Başvuru: 26/11/2024
Düzeltilme: 08/01/2025
Kabul: 05/02/2025

Anahtar Kelimeler

Güneş Destekli Enerji Sistemleri
Organik Rankine Döngüsü
Eksergoekonomik analiz
Parabolik oluk kolektörleri

Öz

Bu çalışma, güneş destekli kombine soğutma, ısıtma ve güç (CCHP) sistemlerinin enerji verimliliği ve sürdürülebilirlik zorluklarını ele alma potansiyelini, özellikle Antalya, Türkiye gibi bol güneş kaynağına sahip bölgelerde araştırmaktadır. Parabolik oluk kolektörleri, organik Rankine çevrimi motoru ve absorpsiyonlu soğutma ünitesini entegre eden bir trijenerasyon sistemi üzerinde termodinamik tasarım ve eksergoekonomik analiz gerçekleştirilmiştir. Engineering Equation Solver (EES) kullanılarak yapılan durağan hal simülasyonları ile R245fa ve bütan olmak üzere iki farklı çalışma akışkanı için termal ve ekserji verimlilikleri, güç çıktıları ve maliyet oranları gibi temel performans ölçütleri değerlendirilmiştir. Sonuçlar, R245fa bazlı sistemin 232,5 kW elektrik üretimi, 716,7 kW soğutma kapasitesi, 2225 kW ısıtma kapasitesi, %86,89 termal verimlilik, %16,26 ekserji verimliliği, 66,12 \$/saat toplam maliyet oranı ve 0,195 kg CO₂/kWh karbon ayak izi sağladığını göstermektedir. Ayrıca, bu sistemin eksergoekonomik faktörü %72,12 olarak hesaplanmıştır. Öte yandan, bütan bazlı sistem 221,8 kW elektrik üretimi, 745,4 kW soğutma kapasitesi, 2197 kW ısıtma kapasitesi, %86,44 termal verimlilik, %15,73 ekserji verimliliği, 63,06 \$/saat toplam maliyet oranı ve 0,223 kg CO₂/kWh karbon ayak izi sağlamıştır. Bütan bazlı sistemin eksergoekonomik faktörü %70,86 olarak hesaplanmıştır. Model doğrulaması için Ortalama Mutlak Yüzde Hata (MAPE) %5'in altında olup, sonuçların güvenilirliğini doğrulamaktadır. Bulgular, R245fa'nın termodinamik ve çevresel ölçütler açısından üstün performans sergilediğini, ancak bütanın maliyet açısından avantaj sunduğunu ortaya koymaktadır.

1. INTRODUCTION (GİRİŞ)

The quest for sustainable energy solutions has intensified amid rising energy demands and climate

change challenges [1]. Solar-assisted Combined Heating, Cooling, and Power (CCHP) systems offer a promising approach, efficiently meeting diverse energy needs with a single adaptable system [2].

These systems deliver heating, cooling, and electricity, providing a comprehensive solution to growing energy consumption [3]. Renewable energy integration is crucial to tackling climate change [4,5]. Solar energy, abundant and eco-friendly, can revolutionize energy systems. Solar-assisted CCHP systems enhance efficiency by providing electricity, heating, and cooling simultaneously [6,7]. Recent advancements in CCHP systems integrated with renewable energy sources have significantly enhanced their efficiency, sustainability, and cost-effectiveness [8]. However, most studies focus on specific applications without providing a holistic thermodynamic and exergoeconomic assessment. For example, Ukaegbu et al. [9] optimized solar-assisted CCHP systems to balance net power, efficiency, and CO₂ emissions but did not explore the economic trade-offs of using different working fluids. Similarly, Liu et al. [10] demonstrated the enhanced efficiency of biomass and natural gas co-firing in a CCHP system, achieving exergy and thermal efficiencies of 41.76% and 75.69%, respectively. Gao et al. [11] developed a cooling-power-desalination cycle using waste heat from diesel exhaust, identifying optimal operating conditions for improved efficiency and cost-effectiveness. Wang et al. [12] introduced an ammonia-water system for low-temperature heat source utilization, achieving thermal and exergy efficiencies of 24.62% and 11.52%, respectively. Zeng et al. [13] optimized solar absorption cooling systems based on meteorological data, reducing the system's total cost rate by 13.6% compared to the base case. Divan et al. [14] proposed a molten carbonate fuel cell-based hybrid system for CCHP applications, reporting energy and exergy efficiencies of 54% and 52.58% with minimal CO₂ emissions. Takleh et al. [15] evaluated solar-geothermal systems using different working fluids, finding that R423A provided the highest energy efficiency and lowest exergy degradation rates. Wang et al. [16] applied energy-based optimization to hybrid solar building CCHP systems, reducing annual energy consumption through optimal component selection. Pokson and Chaiyat [17] designed an IMW-CCHP system utilizing waste heat, achieving exergy and energy efficiencies of 25.88% and 12.25%, respectively, with low energy costs. Al-Sayyab et al. [18] improved cooling COP using alternative refrigerants in a solar-driven heat pump, achieving up to a 75% COP increase with R450A compared to R134a. Yan et al. [19]

optimized hybrid CCHP capacity incorporating geothermal, solar, and wind energy, achieving significant reductions in CO₂ emissions and enhanced energy independence. Ao et al. [20] introduced multi-scenario optimization for hybrid CCHP design, improving computation efficiency and optimizing system flexibility. Wang et al. [21] integrated a CCHP system with full-spectrum solar devices, achieving energy and exergy efficiencies of 70.65% and 26.59%, respectively, with 16% CO₂ reduction. Nami et al. [22] developed a solar-assisted biomass-based trigeneration system for domestic needs, demonstrating high energy efficiency and reliable performance across seasonal conditions. Cavalcanti et al. [23] modeled evacuated tube collectors and absorption chillers, confirming the impact of dead state temperature on exergy efficiency. Wang et al. [24] optimized hybrid CCHP systems under load and RES uncertainties, reducing greenhouse gas emissions while enhancing energy-saving benefits. Saini et al. [25] proposed a solar-driven CCHP system with thermal energy storage for remote buildings, improving exergy efficiency and reducing power and cooling costs. Ramos et al. [26] showed PV-T systems can meet residential energy needs, reducing energy costs by 30–40% compared to PV-only systems. Fani and Sadreddin [27] analyzed solar CCHP systems for office buildings, achieving up to 89% efficiency and reducing CO₂ emissions by 2,217 kg/day in winter.

This research is notable for its novel method of using renewable solar energy in Combined Cooling, Heating, and Power (CCHP) systems to tackle climate change and energy sustainability issues. This study simulates a solar-assisted CCHP system in Antalya, Turkey, assessing the influence of several working fluids, including R245fa and octane, on the efficiency of the ORC and the system's steady-state performance under varied sun intensities.

The study emphasizes the ecological advantages of decreasing carbon emissions and shows the economic efficiency of solar energy in promoting sustainable development. The results provide practical insights for enhancing solar-integrated energy systems, aiding policy formulation, and promoting global initiatives for a low-carbon future. To further clarify the current study's differences and novelty, Table 1 compares methodologies and results from key literature.

Table 1: Comparative Analysis of Methodologies and Key Findings in Solar-Assisted CCHP Studies (Güneş Destekli CCHP Çalışmalarında Metodolojilerin ve Temel Bulguların Karşılaştırmalı Analizi)

Study	Methodology	Key Findings	Differences with Current Study
Ukaegbu et al. [9]	Optimization of solar-assisted CCHP systems	Balanced power, efficiency, and CO ₂ emissions	Did not examine working fluids, economic aspects, or regional specificity (e.g., Antalya's climate)
Liu et al. [10]	Biomass and natural gas co-firing in CCHP	High efficiency achieved with co-firing	No solar integration; focused on biomass and fossil-based fuels
Gao et al. [11]	Cooling-power-desalination combined cycle	Enhanced efficiency with diesel exhaust recovery	Focused on waste heat recovery; no direct comparison of working fluids or thermodynamic specifics
Current Study	Simulation of solar-assisted CCHP with PTCs	Comprehensive thermodynamic, exergoeconomic, and environmental analysis; comparison of R245fa and butane	Novel integration of solar energy with working fluid comparison in a location-specific context

2. MODEL DESCRIPTION (MODEL AÇIKLAMASI)

Solar-assisted CCHP systems integrate solar energy into a hybrid setup to simultaneously produce electricity, heating, and cooling, enhancing energy efficiency and sustainability, as seen in Figure 1. These systems consist of interconnected components, including solar collectors, an Organic Rankine Cycle (ORC) unit, an absorption chiller, and thermal energy storage, each playing a vital role in the system's operation. Parabolic solar collectors focus sunlight onto a receiver containing Therminol 66, a heat transfer fluid, which absorbs thermal energy and transfers it to a thermal storage tank as superheated steam. This stored energy drives the ORC, efficiently generating electricity and thermal energy by utilizing waste heat for heating applications. The residual thermal energy from the ORC powers the absorption chiller, which produces chilled water using a lithium bromide-water solution for cooling processes. Excess thermal energy is stored and utilized later to ensure reliable performance during high-demand periods, optimizing the system's overall effectiveness and reducing energy waste. R245fa and butane were chosen for their advantageous thermodynamic characteristics, rendering them appropriate for use in Organic Rankine Cycle (ORC) systems. R245fa has a low boiling point and exceptional thermal stability, making it optimal for high efficiency in

moderate temperature applications. Conversely, butane is readily accessible, economical, and has significant cooling capability, making it a viable choice for certain applications. The two fluids exhibit different performance trade-offs for efficiency, cost, and environmental effect, offering a thorough foundation for comparison in solar-assisted CCHP systems. Table 1 presents the Input parameters for modeling the solar-assisted CCHP system. The following assumptions are made in the system modeling:

- All components of the system operate under steady-state conditions.
- Therminol-66 oil is used as the working fluid in the solar energy system to transfer heat efficiently from the solar collectors to the storage tank, ARS generator, and ORC evaporator.
- The LiBr-H₂O solution exciting the generator is considered to be in a saturated state.
- The refrigerant vapor leaving the evaporator and the liquid refrigerant exiting the condenser are both assumed to be saturated.
- The throttling valve functions under isenthalpic conditions.
- The effectiveness of the SHEX is assumed to be 0.7.
- Pressure losses within the pipes and heat exchangers are neglected.

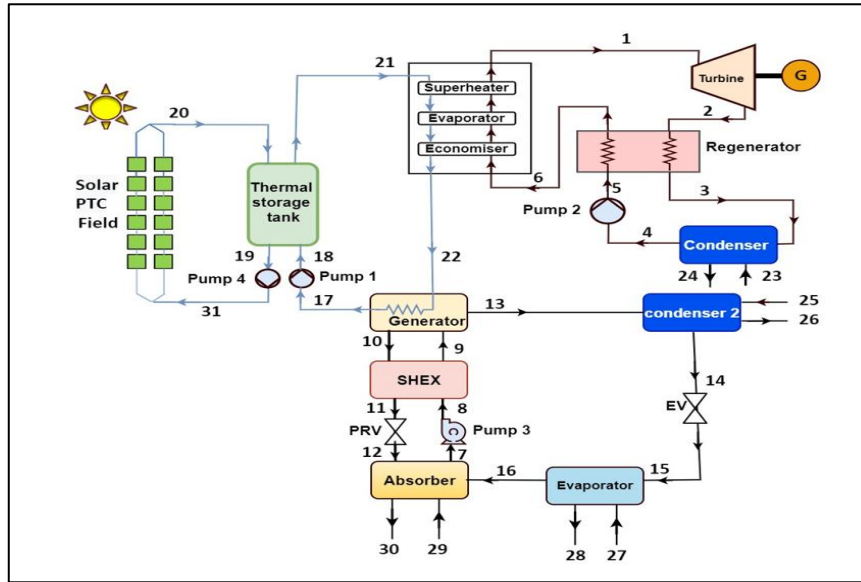


Figure 1. The schematic diagram for solar-assisted CCHP system. (Güneş destekli CCHP sisteminin şematik diyagramı)

Table 2. Input data for modeling the suggested Solar-assisted CCHP system (Önerilen Güneş Destekli CCHP sisteminin modellenmesi için giriş verileri)

Parameter	Value
Solar area	510130 m ²
Sun temperature	5770 K
Solar reservoir outlet temperature	243°C
Solar reservoir inlet temperature	127°C
Latitude (N)	36.54°N
Longitude (E)	30.41°E
Location	Antalya, Turkey
Direct normalC irradiation (DNI)	6.25 kWh/m ² .day
T _{amb}	25°C
P _{amb}	101 kPa
Absorber temperature (T ₁₂)	36°C
Generator temperature (T ₁₅)	90°C
LiBr solution strength	55%
Compressor efficiency	85%
ORC turbine efficiency	90%
ORC pump efficiency	80%

The core equations governing mass, energy, and exergy balances for a control volume while neglecting potential and kinetic energy variations are outlined below. These equations form the basis for modeling the operation of the model:

$$\sum \dot{m}_{in} - \sum \dot{m}_{out} = 0 \quad (1)$$

$$\dot{Q} - \dot{W} + \sum \dot{E}_{in} - \sum \dot{E}_{out} = \frac{dE_{cv}}{dt} \quad (2)$$

$$\dot{E}x_{in} + \dot{E}x_Q - \dot{E}x_{out} - \dot{E}x_W - \dot{E}x_{dis} = 0 \quad (3)$$

Exergy for a thermodynamic system exchanging energy as heat with a reference environment can be defined as [28]:

$$\dot{E}x_Q = \dot{Q}_i \left(1 - \frac{T_0}{T_i} \right) \quad (4)$$

The exergy rate associated with work is equivalent to the rate of energy transfer through work:

$$\dot{E}x_W = \dot{W} \quad (5)$$

The energy transfer rate of a fluid is calculated as:

$$\dot{E}x_{in} = \dot{m}ex_{in} \quad (6)$$

$$\dot{E}x_{out} = \dot{m}ex_{out} \tag{7}$$

Lastly, the following indicators are added to examine the performance of the CCHP system:

Overall output work:

$$\dot{W}_{net} = \dot{W}_{ORT} - \dot{W}_{P1} - \dot{W}_{P2} - \dot{W}_{P3} - \dot{W}_{P4} \tag{8}$$

Overall efficiency:

$$\eta_{CCHP} = \frac{\dot{W}_{net} + \dot{Q}_{heating} + \dot{Q}_{cooling}}{A_{Coll} \cdot \eta_{coll} \cdot DNI \cdot N_{Coll}} \tag{9}$$

$$\Psi_{SCCHP} = \frac{\dot{W}_{net} + \dot{E}X_{P,heating} + \dot{E}X_{P,cooling}}{\dot{Q}_{solar} \left(1 - \frac{T_0}{T_{sun}}\right)} \tag{10}$$

Coefficient of performance

$$COP_{VARS} = \frac{\dot{Q}_{Evaporator}}{\dot{Q}_{Generator} + \dot{W}_{Pump3}} \tag{11}$$

Exergoeconomic analysis evaluates the cost flows, total cost rates, and specific costs associated with the system's exergy streams, including the costs of exergy destruction and exergoeconomic factors. As part of this analysis, cost balances for the kth component are expressed Eq. 12 [29], with the cost rate for the j stream determined using Eq. 13 [30].

$$\sum (c_{in} \dot{E}x_{in})_k + c_{q,k} \dot{E}x_{q,k} + \dot{Z}_k = \sum (c_{out} \dot{E}x_{out})_k + c_{w,k} \dot{W}_k \tag{12}$$

$$\dot{C}_j = c_j \dot{E}x_j \tag{13}$$

The total cost rate for the kth component, encompassing both capital investment and operation and maintenance costs, is expressed in Eq. 14 [31].

$$\dot{Z}_k = z_k * CRF * \frac{\phi}{\tau} \tag{14}$$

Here, τ denotes the annual operating hours, ϕ represents the maintenance factor, and CRF refers to the Capital Recovery Factor as defined in Eq. 15 [32]. Additionally, z_k represents the purchase cost of the kth component. In Eq. 15, i indicates the annual interest rate, while n corresponds to the system's operational lifespan in years.

$$CRF = \frac{i(1+i)^N}{(1+i)^N - 1} \tag{15}$$

To assess the exergoeconomic performance of the kth component, several key parameters must be determined based on the definitions of fuel and product) [33]. These include the average unit cost of fuel (Eq. 16), the average unit cost of the product (Eq. 17), the cost rate of exergy destruction (Eq. 18), and the exergoeconomic factor (Eq. 24). Ultimately, the total unit cost of the product is expressed by Eq. 22 [34]:

$$c_{F,k} = \frac{\dot{C}_{F,k}}{\dot{E}_{F,k}} \tag{16}$$

$$c_{P,k} = \frac{\dot{C}_{P,k}}{\dot{E}_{P,k}} \tag{17}$$

$$\dot{C}_{D,k} = c_{F,k} \dot{E}_{D,k} \tag{18}$$

$$f_k = \frac{\dot{Z}_k}{\dot{Z}_k + \dot{C}_{D,k}} \tag{19}$$

$$\dot{C}_{total} = \frac{\dot{Z}_k + \dot{C}_{D,k}}{\dot{W}_{net} + \dot{Q}_{heating} + \dot{Q}_{cooling}} \tag{20}$$

3. RESULTS (BULGULAR)

The ORC model is validated by comparing its simulation results with those of Delgado-Torres and García-Rodríguez [35] for R245fa. It focuses on an ORC generating 100 kW of electricity with a turbine inlet temperature of 95°C. Table 2 compares the results of the current ORC model with the reference data from Delgado-Torres and García-Rodríguez [35] to validate its accuracy. The turbine inlet temperature (T_1) is identical in both models at 95°C, showing no deviation. The mass flow rate (\dot{m}_{ORC}) exhibits a minor deviation of 4.07%, with the

current model predicting 4.27 kg/s compared to 4.444 kg/s in the reference. The condenser outlet temperature (T_3) shows a slight variation of 0.7%, with the present model reporting 36.67°C versus 36.4°C in the reference. The ORC efficiency (η_{ORC}) is also closely aligned, with a deviation of only 0.5%, where the present model estimates 10.08% compared to 10.14% in the reference. Overall, the results indicate a high degree of agreement, validating the reliability of the present model for simulating ORC performance.

Table 3. Verification of the ORC model by comparing the current model's findings with Ref's [35] (Mevcut model bulgularının Ref'in [35] bulgularıyla karşılaştırılması yoluyla ORC modelinin doğrulanması)

	Ref. [35]	Present model	Deviation (%)
T_1 (°C)	95	95	0
\dot{m}_{ORC} (kg/s)	4.444	4.27	4.07
T_3 (°C)	36.4	36.67	0.7
η_{ORC} (%)	10.14	10.08	0.5

To address the potential instabilities in the absence of direct comparisons with existing studies, an uncertainty analysis was conducted to evaluate the reliability of the results, as seen in Table 4. The analysis employed the root-sum-square (RSS) method to propagate uncertainties from input parameters such as temperature, pressure, and mass flow rate to key output variables, including net work output (\dot{W}_{net}), heating capacity ($\dot{Q}_{heating}$), cooling capacity ($\dot{Q}_{cooling}$), thermal efficiency (η), and

exergy efficiency (ψ). The results revealed uncertainties of $\pm 2.5\%$ for net work output, $\pm 3.2\%$ for heating capacity, and $\pm 3.0\%$ for cooling capacity, which are well within acceptable ranges for thermodynamic simulations. Additionally, uncertainties for thermal and exergy efficiencies were $\pm 1.8\%$ and $\pm 2.1\%$, respectively. These findings confirm the robustness of the model and provide confidence in the reported results, ensuring their reliability despite the absence of comparable systems in the literature.

Table 4. Uncertainty Analysis of Key Performance Parameters (Temel Performans Parametrelerinin Belirsizlik Analizi.)

Parameter	Value (R245fa)	Value (Butane)	Uncertainty (%)
Net work output (\dot{W}_{net})	232.5	2225	$\pm 2.5\%$
Heating capacity ($\dot{Q}_{heating}$)	221.8	2197	$\pm 3.2\%$
Cooling capacity ($\dot{Q}_{cooling}$)	716.7 kW	745.4 kW	$\pm 3.0\%$
Thermal efficiency (η)	86.89%	86.44%	$\pm 1.8\%$
Exergy efficiency (ψ)	6.26%	15.73%	$\pm 2.1\%$

Table 5 comprehensively summarizes energy and exergy performance for each system component, comparing the working fluids R245fa and n-butane in the ORC. The findings highlight several key insights into the system's operation and performance: The absorber exhibits a similar energy input for both fluids, with 884.5 kW for R245fa and 920 kW for n-butane, accounting for around 33.57 kW and 34.92 kW of exergy destruction, respectively. This indicates comparable efficiency in transferring energy between the components for both working fluids. For R245fa, the ORC condenser removes 76.75 kW of energy with an exergy efficiency of 7.18%, while for n-butane, it removes 75.32 kW with an exergy efficiency of 7.21%. The ORC heat exchanger also shows a consistent performance, with slightly lower exergy destruction in the system using n-butane. The heat

removed from the evaporator is higher for n-butane (745.4 kW) compared to R245fa (716.7 kW), indicating slightly better thermal transfer with n-butane. However, both working fluids have similar exergy efficiency for this component, at 54.34%. The boiler's energy input for R245fa (2476 kW) and n-butane (2437 kW) is nearly identical, with R245fa having slightly lower exergy destruction (10.71 kW vs. 16.07 kW). For both fluids, pump efficiency varies slightly, with pump energy consumption being 16.77% of the total power for R245fa and 18.7% for n-butane. The PTC solar collectors exhibit the highest exergy destruction rates for both fluids, with values of 90.06% for R245fa and 90.22% for n-butane. This suggests that the solar collectors remain the most critical component for optimization, as they are responsible for a significant portion of exergy losses. The net work

output of the system is higher for R245fa (232.8 kW) compared to n-butane (221.83 kW). Similarly, the heat supply for R245fa is slightly greater (2225 kW vs. 2197 kW), highlighting that R245fa marginally outperforms n-butane in terms of overall system energy output. While both fluids perform similarly in most components, the system using R245fa demonstrates slightly better exergy efficiency in critical components such as the boiler and pumps. However, n-butane exhibits higher heat removal at the evaporator, making it potentially more suitable for applications requiring higher

cooling capacity. R245fa and n-butane provide comparable performance in the CCHP system, but R245fa slightly outperforms n-butane regarding net work output and process heat supply. However, the higher heat removal in the evaporator for n-butane may make it advantageous for applications requiring enhanced cooling performance. The PTC solar collector remains the component with the highest exergy destruction, underscoring the need for further optimization to improve overall system efficiency.

Table 5. Energy and exergy analysis for each system component for both working fluids (Her iki çalışma akışkanı için her sistem bileşeni için enerji ve ekserji analizi)

Component	R245fa				n-butane			
	$\dot{E}_{D,total}$ (kW)	$\dot{E}_{D,total}$ (%)	Exergy (%)	\dot{Q} or \dot{W} (kW)	$\dot{E}_{D,total}$ (kW)	$\dot{E}_{D,total}$ (%)	Exergy (%)	\dot{Q} or \dot{W} (kW)
Absorber	33.57	0.9472	39.78	884.5	34.92	0.982	39.78	920
ARC cond	9.32	0.263	66.86	749.4	9.7	0.2725	66.86	779.8
Boiler	10.71	0.3023	98.45	2476	16.07	0.452	97.6	2437
EV ₁	2.013	0.057	88.25	0	2.093	0.06	88.25	0
Evap	21.67	0.612	54.34	716.7	22.54	0.634	54.34	745.4
Generator	19.23	0.543	87.41	896.5	20.04	0.564	87.93	932.4
ORC cond	76.75	2.166	80.71	2225	67.21	1.89	82.51	2197
ORC HE	2.305	0.0651	98.2	30.41	1.983	0.0545	98.54	597.2
ORT	23.49	0.663	92.25	279.7	23.03	0.648	92.22	273
Pump ₁	7.338	0.207	16.5	8.79	7.631	0.2146	16.67	9.158
Pump ₂	4.816	0.136	83.63	29.42	5.42	0.1524	83.57	32.98
Pump ₃	0.0385	0.0011	3.313	0.04	0.04	0.001	3.313	0.0414
Pump ₄	7.259	0.205	16.03	8.645	7.55	0.21	16.07	8.995
PRV	0.0452	0.0013	99.98	0	0.047	0.001	99.98	0
PTC	3212	90.63	22.88	4392	3223	90.63	22.6	4392
SHEX	0.1066	0.003	96.36	30.41	0.1109	0.0031	96.36	31.63
TST	113.4	3.2	88.12	3654	114.8	3.227	87.83	3661

Table 6 presents the exergoeconomic analysis of each component in the CCHP system for the working fluids R245fa and n-butane. The findings provide significant insights into the cost distribution, exergoeconomic performance, and areas for improvement for the models. The total cost rate ($\dot{Z}_K + \dot{C}_D$) is slightly higher for R245fa (65.1176 \$/h) compared to n-butane (63.0576 \$/h),

indicating slightly higher economic demand when using R245fa as the working fluid. The total cost associated with exergy destruction (\dot{C}_D) for R245fa (18.162 \$/h) is also marginally higher than for n-butane (18.372 \$/h), suggesting similar performance in terms of minimizing inefficiencies. Components with high exergoeconomic factors (f) include the ORC HE (78.45% for R245fa and

80.84% for n-butane), indicating that a large portion of the cost for this component is driven by capital investment rather than exergy destruction. This highlights its economic efficiency and the importance of its design in the system. Conversely, components like EV1 and PRV have negligible exergoeconomic factors, emphasizing that their costs are almost entirely due to exergy destruction. These components are prime targets for optimization, such as by enhancing heat exchange efficiency or reducing irreversibilities. Heat exchangers (evaporator, condensers, and ORC HE) account for significant portions of both exergy destruction costs and capital investment. The evaporator, for instance, contributes 0.533 \$/h to exergy destruction costs for R245fa and 0.561 \$/h for n-butane. Enhancing these components through improved materials or design could result in substantial economic and thermodynamic performance gains. The ARC condenser shows a similar trend, with \dot{C}_D values of 1.7 \$/h and 1.788 \$/h for R245fa and n-butane, respectively, suggesting comparable inefficiencies for both working fluids. The turbines (ORT) demonstrate relatively high exergoeconomic factors (75.66% for R245fa and 57.54% for n-butane), indicating that capital investment significantly influences their costs. However, further improvements in isentropic efficiency could reduce exergy destruction, thereby lowering operational costs. Pumps exhibit varying levels of performance, with Pump 4 showing higher exergoeconomic factors (69.55% for R245fa and 72.22% for n-butane). In contrast, other pumps like Pump 1 and Pump 2 demonstrate relatively low values, highlighting the need for efficiency improvements. The PTC solar collector is a critical component, as it has the highest capital investment costs for both working fluids (39.22 \$/h for both R245fa and n-butane). Its exergoeconomic factor is 100% for both cases, indicating that all associated costs are tied to capital investment. The slightly higher exergoeconomic factor for R245fa (72.11%) compared to n-butane (70.86%) reflects marginally better economic performance, likely due to lower operational inefficiencies in key components. The generator's cost rates (cd) are 0.94 \$/h for R245fa and 0.9933 \$/h for n-butane, with exergoeconomic factors of 45.85% for both fluids. This parity suggests similar behavior of the generator across working fluids, making it a stable component in the system.

Table 7 summarizes the energy, exergy, and exergoeconomic performance of the CCHP system using R245fa and n-butane as working fluids. The results present the R245fa demonstrates superior performance in terms of network output, heating

capacity, exergy efficiency, and CO₂ emissions, making it a better choice for systems focusing on power generation and heating with lower environmental impact. n-butane shows a higher cooling capacity and lower operational cost, making it more suitable for applications prioritizing cooling or cost-efficiency. The marginal differences in thermal efficiency and exergy destruction between the two fluids suggest that either option can be viable depending on the specific application priorities. Optimization of components with high exergy destruction, such as the heat exchangers and the ORC subsystem, can further enhance the system's overall efficiency and cost-effectiveness for both fluids. The net power output is slightly higher for R245fa (232.5 kW) compared to n-butane (221.8 kW). This indicates that R245fa performs better in terms of electricity generation, likely due to its thermodynamic properties leading to higher efficiency in the turbine. The heating output (\dot{Q}_{heating}) is higher for R245fa (2225 kW) than for n-butane (2197 kW), indicating better performance for heating applications with R245fa. Conversely, the cooling capacity (\dot{Q}_{cooling}) is greater for n-butane (745.4 kW) compared to R245fa (716.7 kW). This makes n-butane a more suitable choice for applications prioritizing cooling. The thermal efficiency of the system is almost identical for both working fluids, with R245fa achieving 86.89% and n-butane achieving 86.44%. This indicates that both fluids utilize the input energy effectively with minimal differences. The exergy efficiency (ψ) is slightly higher for R245fa (16.26%) compared to n-butane (15.73%). This suggests that R245fa has a slight advantage in converting available exergy into useful work and heat, indicating better overall system performance in terms of thermodynamic efficiency. The total exergy destruction is marginally lower for R245fa (3544 kW) compared to n-butane (3557 kW). Although the difference is minimal, it reflects a slightly more efficient energy utilization with R245fa. The total cost rate is slightly higher for R245fa (66.12 \$/h) compared to n-butane (63.06 \$/h). While R245fa provides better thermodynamic performance, it comes with a marginally higher operational cost. The exergoeconomic factor (f) is higher for R245fa (72.12%) compared to n-butane (70.86%). This indicates that for R245fa, a larger proportion of the total cost is associated with capital investment rather than the cost of exergy destruction, highlighting its economic feasibility. The CO₂ emissions are significantly lower for R245fa (0.195 kg/kWh) compared to n-butane (0.223 kg/kWh), making R245fa a more environmentally friendly choice for the system.

Table 6. Exergoeconomic analysis for each component of the CCHP system for both working fluids (Her iki çalışma sıvısı için CCHP sisteminin her bir bileşeni için eksergoekonomik analiz)

Component	R245fa				n-butane			
	\dot{C}_D (\$/h)	\dot{Z}_K (\$/h)	$\dot{Z}_K + \dot{C}_D$ (\$/h)	f %	\dot{C}_D (\$/h)	\dot{Z}_K (\$/h)	$\dot{Z}_K + \dot{C}_D$ (\$/h)	f %
Absorber	2.603	0.208	2.811	7.4	2.742	0.214	2.956	7.24
ARC cond	1.7	0.006	1.706	0.352	1.788	0.009	1.797	0.5
Boiler	0.5236	0.2802	0.8038	34.86	0.7963	0.2837	1.08	26.27
EV ₁	0.367	0.0003	0.3673	0.082	0.3863	0.0006	0.3869	0.155
Evap	0.533	0.379	0.912	41.56	0.561	0.3883	0.9493	40.9
Generator	0.94	0.796	1.736	45.85	0.9933	0.8277	1.821	45.45
ORC cond	4.065	0.426	4.491	9.486	3.632	0.217	3.849	5.64
ORC HE	0.1221	0.4444	0.5665	78.45	0.1047	0.4418	0.5465	80.84
ORT	1.244	3.866	5.11	75.66	1.244	1.686	2.93	57.54
Pump ₁	0.5226	0.2578	0.7804	33.03	0.4943	0.2655	0.7598	34.94
Pump ₂	0.25	0.6057	0.8557	70.78	0.2535	0.6592	0.9127	72.22
Pump ₃	0.0027	0.0056	0.00833	67.59	0.0026	0.0057	0.0083	68.67
Pump ₄	0.517	0.255	0.772	33.03	0.489	0.2621	0.7511	34.89
PRV	0.0023	0.0027	0.005	54	0.0024	0.0029	0.00527	54.46
PTC	0	39.22	39.22	100	0	39.22	39.22	100
SHEX	0.0055	0.0067	0.01223	55.03	0.0058	0.007	0.01275	54.67
TST	4.764	0.196	4.96	3.95	4.877	0.195	5.072	3.84
Total	18.162	46.96	65.11726	72.11	18.372	44.685	63.0576	70.86

Table 7. Summary of the Energy, exergy, and exergoeconomic results of the CCHP system for both organic fluids (Her iki organik akışkan için CCHP sisteminin Enerji, ekserji ve eksergoekonomik sonuçlarının özeti)

Working Fluid	\dot{W}_{net} (kW)	$\dot{Q}_{heating}$ (kW)	$\dot{Q}_{cooling}$ (kW)	η (%)	ψ (%)	$\dot{E}_{D,total}$ kW	\dot{C}_{total} \$/h	f %	CO ₂ emission (kg/kWh)
R245fa	232.5	2225	716.7	86.89	16.26	3544	66.12	72.12	0.195
butane	221.8	2197	745.4	86.44	15.73	3557	63.06	70.86	0.223

Figure 2 illustrates the net output power (\dot{W}_{net}) and total cost rate (\dot{C}_{Total}) as a function of the superheated degree at the ORC intake for the system with two working fluids. The findings present that the work net increases with an increase in the superheating degree, whereas the total cost decreases. The \dot{W}_{net} for the CCHP system with R245fa is more significant than with butane. It is noticed from the curves when ΔT_{super} increases

from 5 to 50 °C, the \dot{W}_{net} increases from 174.6 to 294.3 kW for the system with butane, while it rises from 185.1 to 304 kW for the system with R245fa. Conversely, the total cost rate (\dot{C}_{Total}) for the CCHP system with butane is more attractive than the system with R245fa because the mass flow rate of the ORC with R245fa is higher than for the ORC with butane, and it causes an increase in the total cost investment for the components of the ORC.

The \dot{C}_{Total} reduces from 66.79 to 63.69 \$/h for the system with R245fa, while it decreases from 64.9 to 61.4 \$/h for the system with butane.

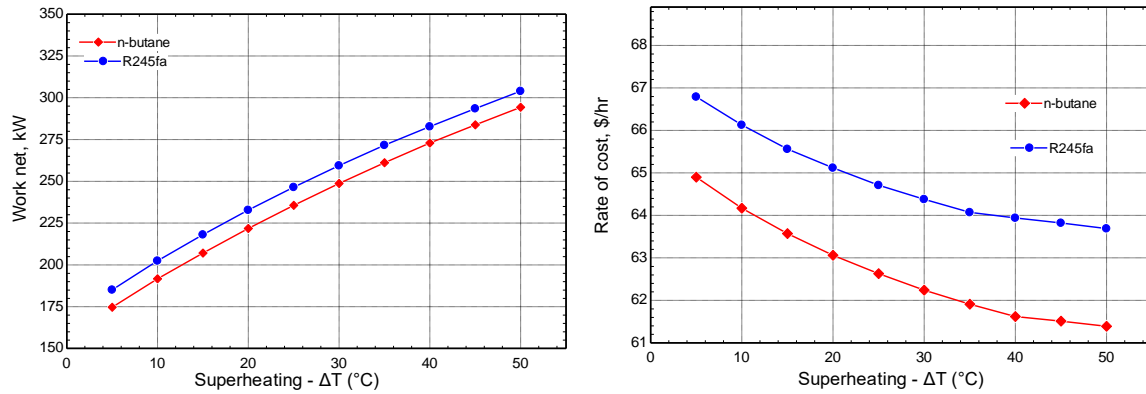


Figure 2. Work net and total cost rate for different superheated degree parameters (Farklı aşırı ısıtma dereceleri için iş net ve toplam maliyet oranı)

Figure 3 presents the overall efficiencies of the CCHP system as a function of the superheated degree with two working fluids. It revealed from the curves both the thermal and exergy efficiency of the system increased with an increase in the ΔT_{super} due to the enhancement of the system output (\dot{W}_{net} and $\dot{Q}_{heating}$) at high ΔT_{super} . Compared to the butane-based system, the CCHP

system that uses R245fa achieves higher overall efficiency. The $\eta_{thermal}$ enhances from 85.13 to 89.5 % and the η_{exergy} increases from 14.8 to 18.32 % for the system with R245fa when ΔT_{super} increases from 5 to 50 °C. Also, the $\eta_{thermal}$ enhances from 84.59 to 89.21 % and the η_{exergy} increases from 14.25 to 17.85 % for the system with butane.

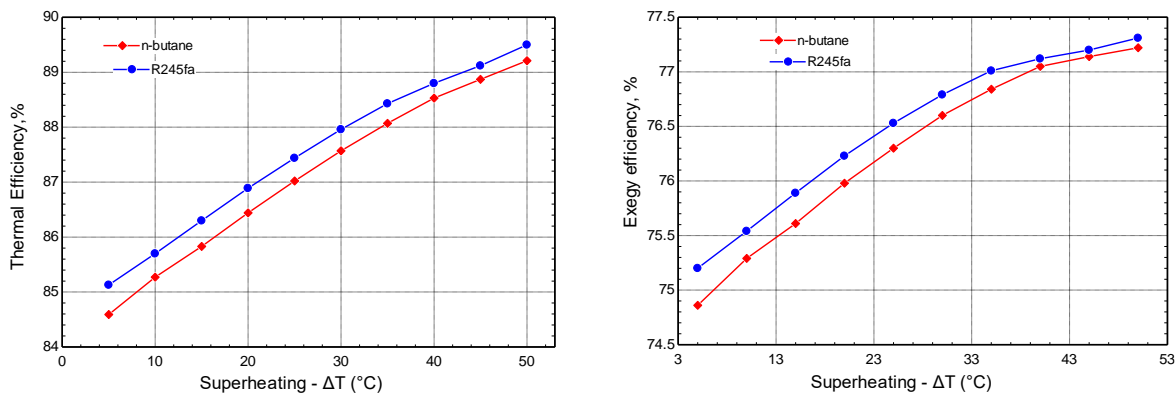


Figure 3. Overall efficiencies of the CCHP system for different superheated degree parameters (Farklı aşırı ısıtma derecesi parametreleri için CCHP sisteminin genel verimlilikleri)

The pressure ratio (α) represents the relationship between the turbine intake pressure (P_1) and the critical pressure ($P_{critical}$) of the working fluid. For R245fa, the critical pressure is 3651 kPa, whereas for butane, it is 3797 kPa. The effect of the pressure ratio parameter on the \dot{W}_{net} and \dot{C}_{Total} of the CCHP system are shown in Figure 4. The results indicate that the \dot{W}_{net} rises as the pressure ratio increases, but the overall cost \dot{C}_{Total} reduces. The \dot{W}_{net} production of the CCHP system using R245fa is higher, while the overall cost \dot{C}_{Total} is more expensive than using butane. It can be seen from the graphs that when the α value goes from 0.5 to 0.8, the \dot{W}_{net} increases from 96.83 kW to 240.8 kW for

the system using butane, and from 121.8 kW to 249.6 kW for the system using R245fa. The \dot{C}_{Total} reduces from 68.67 \$/h to 64.74 \$/h for the system with R245fa, while it decreases from 68.61 \$/h to 62.46 \$/h for the system with butane.

The overall efficiencies of the system as a function of the pressure ratio with two working fluids are presented in Figure 5. At a high-pressure ratio (α), the \dot{W}_{net} and $\dot{Q}_{heating}$ increase and cause an enhancement in the overall efficiencies of the system for both fluids. The CCHP system with R245fa demonstrates superior overall efficiency compared to the butane-based system. When the

pressure ratio (α) increases from 0.5 to 0.8, the η_{thermal} improves from 84.19 to 87.28% and the η_{exergy} increases from 13.28 to 16.7% for the system using R245fa. Similarly, for the system

using butane, the η_{thermal} increases from 83.13 to 86.89% and the η_{exergy} increases from 12.3 to 16.23%.

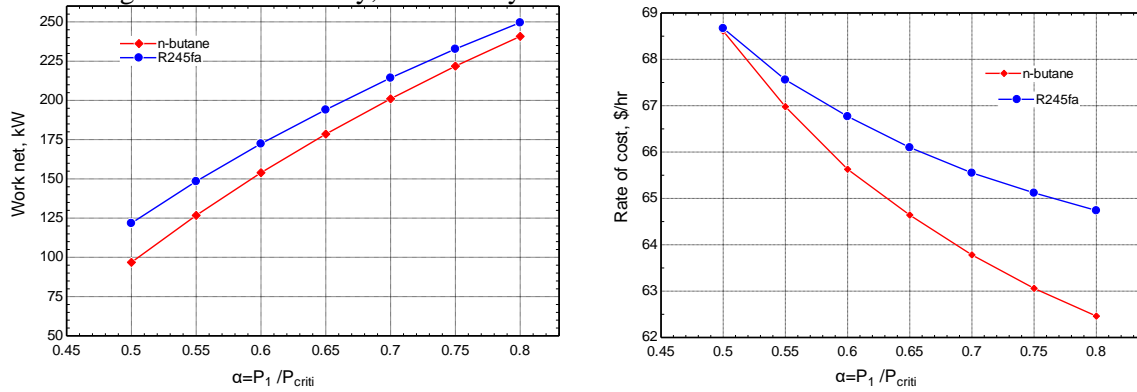


Figure 4. Work net and total cost rate for different pressure ratio parameters (Farklı basınç oranı parametreleri için iş net ve toplam maliyet oranı)

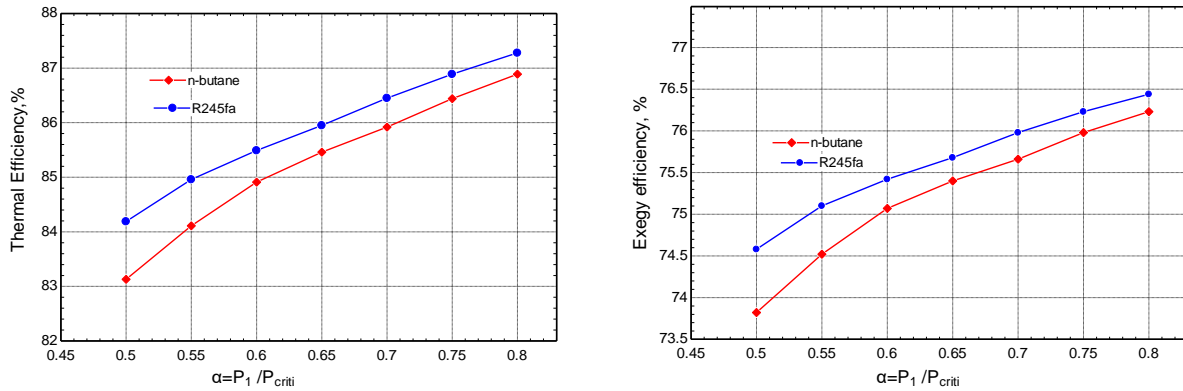


Figure 5. Overall efficiencies of the system for different pressure ratio parameters (Farklı basınç oranı parametreleri için sistemin genel verimlilikleri)

4. CONCLUSIONS (SONUÇLAR)

This study conducted a comprehensive analysis of a solar-assisted Combined Cooling, Heating, and Power (CCHP) system, integrating parabolic trough collectors (PTCs) and an Organic Rankine Cycle (ORC). Two working fluids, R245fa and butane, were evaluated for their thermodynamic, exergoeconomic, and environmental performance under steady-state conditions. The findings contribute to advancing the understanding and design of solar-assisted energy systems, particularly in regions with abundant solar resources like Antalya, Turkey. A reliable numerical model was developed for thermodynamic and exergoeconomic evaluation, demonstrating the ability to predict system performance accurately. R245fa was identified as the superior working fluid for thermodynamic and environmental performance, achieving higher efficiencies and a lower carbon footprint. Butane, however, demonstrated cost advantages and a higher cooling capacity, making it suitable for specific applications. The study tailored the system to Antalya's climatic conditions,

highlighting the viability of location-specific solutions for optimizing solar energy utilization.

Future research should focus on several key directions to build on the findings of this study. Expanding the analysis to include dynamic and seasonal conditions would enhance the real-world applicability of the results. Exploring alternative working fluids and innovative system configurations could further improve energy efficiency and cost-effectiveness. Additionally, conducting experimental validation to complement the numerical simulations would strengthen the practical relevance and reliability of the findings. Lastly, investigating hybrid systems that integrate other renewable energy sources, such as wind or geothermal, could diversify and enhance overall system performance, offering more sustainable and adaptable solutions.

SYMBOLS AND ABBREVIATIONS INDEX (SEMBOLLER VE KISALTMALAR DİZİNİ)

SYMBOLS

\dot{C}	Cost Rate (\$/h)
c	Exergy cost per unit (\$/GJ)
\dot{E}	Energy (kW)
$\dot{E}X$	Exergy flows (kW)
f	Exergoeconomic factor (%)
h	Specific enthalpy (kJ/kg)
\dot{m}	Mass flow rate (kg/s)
\dot{Q}	Heat transfer (kW)
\dot{W}	Work done (kW)
Z	Initial cost rate (\$/h)
η	Efficiency (%)
τ	Operation hour (h)
φ	Maintenance factor
ψ	Exergy efficiency (%)

ABBREVIATIONS

Abs	Absorber
ARC	Absorption refrigeration cycle
CCHP	Combined cooling heating power
Comp	Compressor
Cond	Condenser
EV	Expansion valve
Evap	Evaporator
Gen	Generator
HE	Heat exchanger
HRSG	Heat recovery steam generation
ORC	Organic Rankine cycle
ORT	Organic Rankine turbine
P	Pump
PTC	Parabolic trough collectors
RES	Renewable energy sources
SHES	Sensible heat exchanger
TST	Thermal storage tank

DECLARATION OF ETHICAL STANDARDS (ETİK STANDARTLARIN BEYANI)

The authors of this article declares that the materials and methods they use in their work do not require ethical committee approval and/or legal-specific permission.

Bu makalenin yazarı çalışmalarında kullandıkları materyal ve yöntemlerin etik kurul izni ve/veya yasal-özel bir izin gerektirmediğini beyan ederler.

AUTHORS' CONTRIBUTIONS (YAZARLARIN KATKILARI)

Abdulrazzak AKROOT: He conducted the conceptualization, developed the software, analyzed the results, wrote the original draft, and performed review & editing.

Konsept geliştirmeyi gerçekleştirdi, yazılımı geliştirdi, sonuçları analiz etti, orijinal taslağı yazdı ve gözden geçirme ve düzenleme işlemlerini yaptı.

Mohammed REFAEI: He conducted the investigation, methodology, formal analysis, and contributed to writing the original draft.

Araştırmayı, metodolojiyi ve resmi analizi gerçekleştirdi ve orijinal taslağın yazımına katkıda bulundu.

CONFLICT OF INTEREST (ÇIKAR ÇATIŞMASI)

There is no conflict of interest in this study.

Bu çalışmada herhangi bir çıkar çatışması yoktur.

REFERENCES (KAYNAKLAR)

- [1] Lior N. Sustainable energy development: the present (2009) situation and possible paths to the future, *Energy*, 35 (2010) 3976–94.
- [2] Zhang L, Li F, Sun B, Zhang C. Integrated optimization design of combined cooling, heating, and power system coupled with solar and biomass energy, *Energies*, 12 (2019) 687-702.
- [3] Li Y, Kong X. Introduction to CCHP Systems. In: Wang R, Zhai X, editors. *Handbook of Energy Systems in Green Buildings*, Berlin, Heidelberg: Springer Berlin Heidelberg; (2018) 551–572.
- [4] Talal W, Akroot A. Exergoeconomic Analysis of an Integrated Solar Combined Cycle in the Al-Qayara Power Plant in Iraq, *Processes*, 11 (2023) 622-641.
- [5] Talal W, Akroot A. An Exergoeconomic Evaluation of an Innovative Polygeneration System Using a Solar-Driven Rankine Cycle Integrated with the Al-Qayyara Gas Turbine Power Plant and the Absorption Refrigeration Cycle. *Machines*, 12 (2024) 133-148.
- [6] Salimi M, Hosseinpour M, Mansouri S, N. Borhani T. Environmental aspects of the combined cooling, heating, and power (CCHP) systems: a review, *Processes*, 10 (2022) 711-723.
- [7] Assareh E, Dejdard A, Ershadi A, Jafarian M, Mansouri M, Salek roshani A, et al. Performance analysis of solar-assisted-geothermal combined cooling, heating, and

- power (CCHP) systems incorporated with a hydrogen generation subsystem, *Journal of Building Engineering*, 65 (2023) 105727.
- [8] Wang J, Han Z, Guan Z. Hybrid solar-assisted combined cooling, heating, and power systems: A review, *Renewable and Sustainable Energy Reviews*, 133(2020) 110256.
- [9] Ukaegbu U, Tartibu L, Lim CW. Multi-Objective Optimization of a Solar-Assisted Combined Cooling, Heating and Power Generation System Using the Greywolf Optimizer, *Algorithms*, (2023) 16.
- [10] Liu J, Ren J, Zhang Y, Huang W, Xu C, Liu L. Exergoeconomic Evaluation of a Cogeneration System Driven by a Natural Gas and Biomass Co-Firing Gas Turbine Combined with a Steam Rankine Cycle, Organic Rankine Cycle, and Absorption Chiller, *Processes*, 12 (2023) 82.
- [11] Gao Q, Zhao S, Zhang Z, Zhang J, Zhao Y, Sun Y, et al. Performance Analysis and Multi-Objective Optimization of a Cooling-Power-Desalination Combined Cycle for Shipboard Diesel Exhaust Heat Recovery, *Sustainability*, 15 (2023) 16942.
- [12] Wang H, Wang J, Liu Z, Chen H, Liu X. Thermodynamic Analysis of a New Combined Cooling and Power System Coupled by the Kalina Cycle and Ammonia–Water Absorption Refrigeration Cycle, *Sustainability*, 14 (2022) 688 -703.
- [13] Zeng J, Li Z, Peng Z. Exergoeconomic analysis and optimization of solar assisted hybrid cooling systems in full working conditions, *Appl Therm Eng*, 206 (2022) 118082.
- [14] Divan A, Zahedi A, Mousavi SS. Conceptual design and technical analysis of a hybrid natural gas/molten carbonate fuel cell system for combined cooling, heating, and power applications, *Energy*, 273 (2022)112402.
- [15] Rostamnejad Takleh H, Zare V, Mohammadkhani F, Sadeghiasad MM. Proposal and thermoeconomic assessment of an efficient booster-assisted CCHP system based on solar-geothermal energy, *Energy*, 246 (2022) 123360.
- [16] Wang J, Wang J, Yang X, Xie K, Wang D. A novel energy-based optimization model of a building cooling, heating and power system, *Energy Convers Manag*, 268 (2022) 115987.
- [17] Pokson C, Chaiyat N. Thermal performance of a combined cooling, heating, and power (CCHP) generation system from infectious medical waste, *Case Studies in Chemical and Environmental Engineering*, 6 (2022) 1144-1162.
- [18] Khalid Shaker Al-Sayyab A, Mota-Babiloni A, Navarro-Esbrí J. Novel compound waste heat-solar driven ejector-compression heat pump for simultaneous cooling and heating using environmentally friendly refrigerants, *Energy Convers Manag*, 228 (2021) 914-930.
- [19] Yan R, Lu Z, Wang J, Chen H, Wang J, Yang Y, et al. Stochastic multi-scenario optimization for a hybrid combined cooling, heating and power system considering multi-criteria, *Energy Convers Manag*, 233 (2021) 113911.
- [20] Ao X, Liu J, Hu M, Zhao B, Pei G. A rigid spectral selective cover for integrated solar heating and radiative sky cooling system, *Solar Energy Materials and Solar Cells*, 230 (2021) 111270.
- [21] Wang J, Han Z, Liu Y, Zhang X, Cui Z. Thermodynamic analysis of a combined cooling, heating, and power system integrated with full-spectrum hybrid solar energy device, *Energy Convers Mana*, 228 (2021) 113596.
- [22] Nami H, Anvari-Moghaddam A, Nemati A. Modeling and analysis of a solar boosted biomass-driven combined cooling, heating and power plant for domestic applications, *Sustainable Energy Technologies and Assessments*, 47 (2021) 101326.
- [23] Cavalcanti EJC, Ferreira JVM, Carvalho M. Exergy assessment of a solar-assisted combined cooling, heat and power system, *Sustainable Energy Technologies and Assessments*, 47 (2021).
- [24] Wang J, Qi X, Ren F, Zhang G, Wang J. Optimal design of hybrid combined cooling, heating and power systems considering the uncertainties of load demands and renewable energy sources, *J Clean Prod*, 281 (2021)125357.
- [25] Saini P, Singh J, Sarkar J. Thermodynamic, economic and environmental analyses of a novel solar energy driven small-scale combined cooling, heating and power system, *Energy Convers Manag*, 226 (2020) 113542.
- [26] Ramos A, Chatzopoulou MA, Guarracino I, Freeman J, Markides CN. Hybrid photovoltaic-thermal solar systems for combined heating, cooling and power provision in the urban environment, *Energy Convers Manag*, 150 (2017) 838–50.
- [27] Fani M, Sadreddin A. Solar assisted CCHP system, energetic, economic and environmental analysis, case study, Educational office buildings. *Energy Build*, 136 (2017)100–109.

- [28] Khoshgoftar Manesh MH, Mousavi Rabeti SA, Nourpour M, Said Z. Energy, exergy, exergoeconomic, and exergoenvironmental analysis of an innovative solar-geothermal-gas driven polygeneration system for combined power, hydrogen, hot water, and freshwater production, *Sustainable Energy Technologies and Assessments*, 51 (2022).
- [29] Alfari A, Akroot A, Deniz E. The Exergo-Economic and Environmental Evaluation of a Hybrid Solar–Natural Gas Power System in Kirkuk, *Applied Sciences*, 14 (2024) 10113.
- [30] Bakhshmand SK, Saray RK, Bahlouli K, Eftekhari H, Ebrahimi A. Exergoeconomic analysis and optimization of a triple-pressure combined cycle plant using evolutionary algorithm, *Energy*, 93 (2015) 555–67.
- [31] Han Z, Wang J, Cui Z, Lu C, Qi X. Multi-objective optimization and exergoeconomic analysis for a novel full-spectrum solar-assisted methanol combined cooling, heating, and power system, *Energy*, 237 (2021) 121537.
- [32] Akroot A, Al Shammre AS. Economic and Technical Assessing the Hybridization of Solar Combined Cycle System with Fossil Fuel and Rock Bed Thermal Energy Storage in Neom City, *Processes*, 12 (2024) 1433.
- [33] Akroot A, Al Shammre AS. Techno-Economic and Environmental Impact Analysis of a 50 MW Solar-Powered Rankine Cycle System, *Processes*, 12 (2024) 1059.
- [34] Khaljani M, Khoshbakhti Saray R, Bahlouli K. Comprehensive analysis of energy, exergy and exergo-economic of cogeneration of heat and power in a combined gas turbine and organic Rankine cycle, *Energy Convers Manag*, 97 (2015)154–165.
- [35] Delgado-Torres AM, García-Rodríguez L. Analysis and optimization of the low-temperature solar organic Rankine cycle (ORC), *Energy Convers Manag*, 51 (2010) 2846–2856.